Progress In Electromagnetics Research C, Vol. 136, 51–60, 2023

Highly Selective UWB BPF with Dual Notched Bands Using Split Ring Resonator

Guang Yong Wei[1], Yun Xiu Wang[1, *], Jie Liu[2], Yang Gao[1], and Xiao Tao Yao[1]

Abstract—This paper proposes a dual notches ultra-wideband (UWB) bandpass filter (BPF) with high selectivity and wide stopband. It is composed of a multi-mode resonator (MMR) known as a double-T-shaped open stub-loaded MMR, a pair of interdigital coupled lines, and folded split ring resonator. The MMR is designed to place the resulting resonant modes within the UWB passband, then add interdigital coupled lines to achieve strong coupling, resulting in a flat passband. Afterward, multiple complimentary folded split ring resonators (CFSRRs) and folded split ring resonators (FSRRs) are embedded into the designed basic UWB filter to develop dual notches at the desired frequency. The filter is simulated and manufactured using low-cost high-frequency dielectric substrate F4BM. The measurement results agree well with the simulation data. Multiple notches centered on 5.8 and 8 GHz effectively suppress unwanted signals from 5.8 GHz WLAN and 8 GHz satellite systems simultaneously. In addition, two transmission zeros on both sides of the passband are located at 2.7 GHz and 10.76 GHz, respectively, so that the sharp skirt selectivity is improved to 0.857. The measured filter can exhibit high sharp selectivity and wider stopband at the same time.

1. INTRODUCTION

In response to the Federal Communications Commission's (FCC) designation of the 3.1–10.6 GHz band as license-free for indoor communication applications [1], numerous ultra-wideband (UWB) filters have emerged, employing a diverse range of topologies. As crucial components within UWB systems, these filters play a pivotal role in determining communication quality. Consequently, a plethora of UWB filter designs, featuring various techniques and structures, have been documented in the literature, including tapered transmission line resonators [2], multi-mode resonator [3], fractal tree stub [4], circular stub [5], microstrip-to-coplanar waveguide (CPW) transition technology [6–9], and wave cancellation technology [10].

Meanwhile, to mitigate the interference from unwanted narrowband RF signals originating from wireless local area network (WLAN) applications and other radio systems, dual-band or multi-band UWB-BPFs are typically favored in real-world scenarios, as demonstrated in [11–17]. For instance, a UWB-BPF featuring a notched band at 5.2 GHz was presented in [11], achieved by coupling two sets of half-wavelength high-impedance line resonators. In [12], a UWB-BPF was developed using a ring resonator loaded with two open stubs, while a wide notched band filtering effect at 5–6 GHz was accomplished by incorporating a pair of via-loaded ring resonators. To improve the attenuation capabilities of the notched band, a study in [13] proposed a UWB-BPF design that employed a short-circuited L-shaped resonator combined with a slow-wave half-mode substrate-integrated waveguide (SW-HMSIW), resulting in a 5.83 GHz notched band with a depth of 17.9 dB. However, this approach increased the complexity of the UWB filter design due to the numerous through holes required by the

Received 7 June 2023, Accepted 1 August 2023, Scheduled 11 August 2023
* Corresponding author: Yun Xiu Wang (627662147@qq.com).
[1] School of Electronic and Information Engineering, China West Normal University, Nanchong 637009, China. [2] School of Physics and Astronomy, China West Normal University, Nanchong 637009, China.

technology. To reduce its size, [14, 15] leveraged microstrip line coplanar technology and integrated a modified ring resonator to achieve two notches. Similarly, [16, 17] utilized defect ground structures (DGSs) to create double notches. Nonetheless, the structures proposed by [11–17] tend to be overly intricate.

Addressing the challenge of designing more intricate structures with enhanced suppression capabilities, this paper presents a simple and highly selectivity ultra-wideband bandpass filter (UWB-BPF) featuring dual notches. The innovative filter design employs a stub-loaded multimode resonator, which is connected to interdigital coupled lines, ensuring a flat and extensive passband performance. To effectively mitigate interference from wireless narrowband signals, two pairs of resonators are strategically integrated into the feedlines position, generating the desired notches. The proposed filter is realized and optimized utilizing an F4BM substrate with a loss tangent of 0.001, a height of 0.8 mm, and a relative dielectric constant of 3.38.

2. DESIGN OF PROPOSED UWB BPF

The layout of the proposed BPF is depicted in Figure 1. From it, we observe that the middle position of the filter is formed by a novel multimode resonator, which is the basis for constructing a dual notches filter. A UWB filter is created by interdigital coupled lines between the MMR and the 50 Ω feedlines. Later, CFSRR and FSRR were incorporated into it to provide numerous passband notches. Considering that the wideband characteristics of the proposed UWB-BPF are mainly introduced by using a double-T-shaped open stub-loaded (DTOS) multimode resonator (MMR), it is analyzed first. It has a symmetrical construction, and Figure 2 depicts the even-odd mode equivalent circuits for the DTOS MMR.

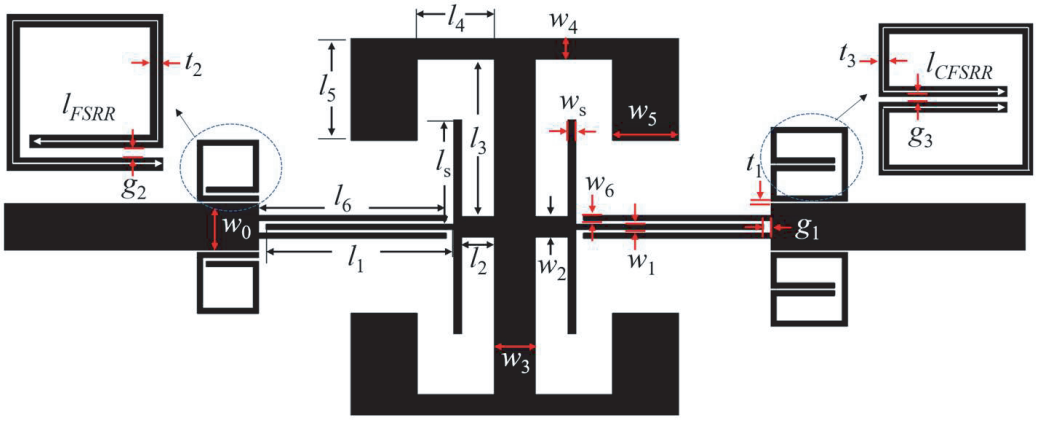

Figure 1. The architecture of the proposed dual notched band UWB filter.

As depicted in Figure 2(a), the MMR is symmetric about the plane A-$A*$, wherein θ_1-θ_5 and θ_s represent the electronic lengths, and they correspond to the characteristic admittances of Y_1-Y_5, and Y_s, respectively. The corresponding circuit for the odd mode is depicted in Figure 2(b), where the symmetrical plane is shorted to the ground. Consequently, the odd mode input admittance can be readily calculated as

$$Y\text{in, odd} = Y_1 \frac{Y_{o1} + jY_1 \tan\theta_1}{Y_1 + jY_{o1} \tan\theta_1} \tag{1}$$

where

$$Y_{o1} = -jY_2 \cot\theta_2 + 2jY_s \tan\theta_s \tag{2}$$

representing the open stubs of the input admittance Y_s and the shorted stub of the input admittance Y_2 parallel connection with each other.

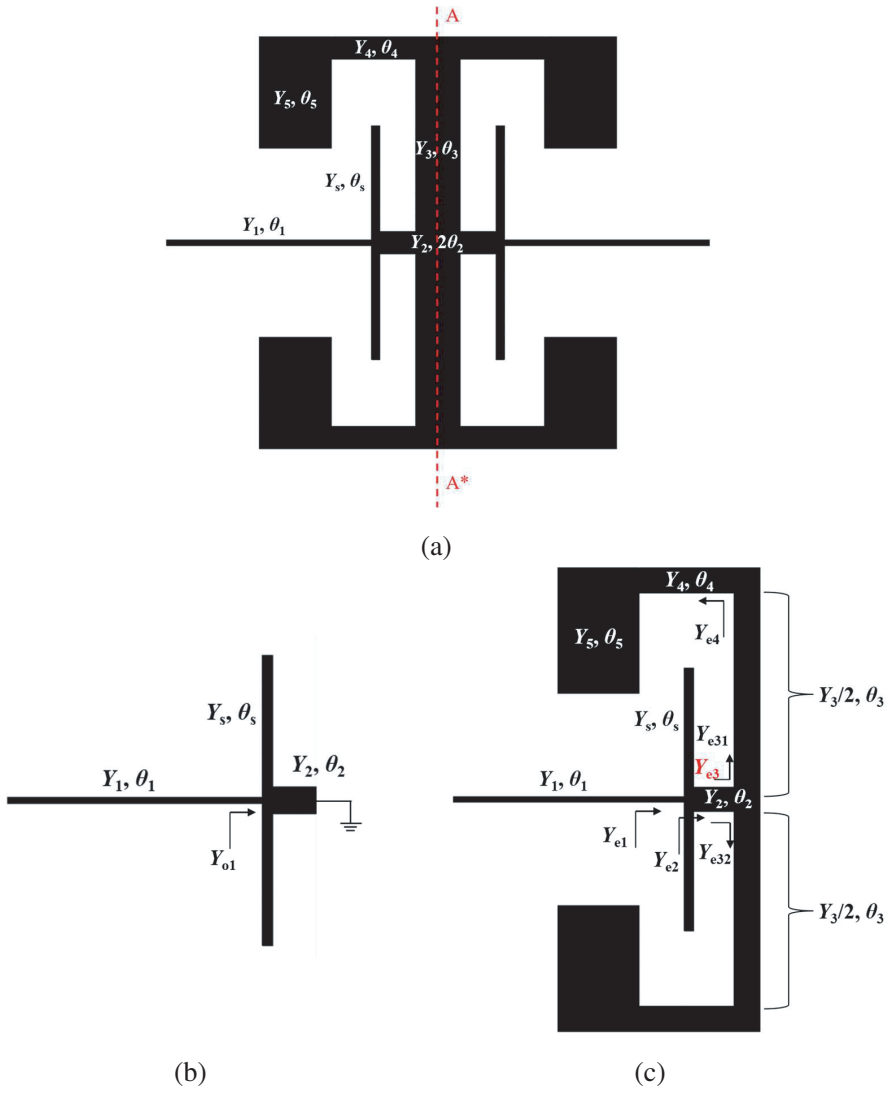

Figure 2. (a) The architecture of the proposed DTOS MMR. (b) Odd-mode equivalent circuit for the MMR. (c) Even-mode equivalent circuit for the MMR.

By resolving $Y_{\text{in,odd}} = 0$, which results from the resonance condition, one may get the odd mode resonance conditions:

$$Y_1 \tan\theta_1 - Y_2 + 2Y_s \tan\theta_s \tan\theta_2 = 0 \tag{3}$$

In a similar manner, the even mode input admittance of the equivalent circuit illustrated in Figure 2(c) can be expressed as follows:

$$Y_{\text{in,even}} = Y_1 \frac{Y_{\text{el}} + jY_1 \tan\theta_1}{Y_1 + jY_{\text{el}} \tan\theta_1} \tag{4}$$

$$Y_{\text{e1}} = Y_{\text{e2}} + 2jY_s \tan\theta_s \tag{5}$$

$$Y_{\text{e2}} = Y_2 \frac{Y_{\text{e3}} + jY_2 \tan\theta_2}{Y_2 + jY_{\text{e3}} \tan\theta_2} \tag{6}$$

$$Y_{\text{e3}} = Y_{\text{e31}} + Y_{\text{e32}} = 2Y_{\text{e31}} = 2\frac{Y_3}{2} \frac{Y_{\text{e4}} + j\dfrac{Y_3}{2} \tan\theta_3}{\dfrac{Y_3}{2} + jY_4 \tan\theta_3} \tag{7}$$

$$Y_{e4} = Y_4 \frac{jY_5 \tan\theta_5 + jY_4 \tan\theta_4}{Y_4 - Y_5 \tan\theta_4 \tan\theta_5} \tag{8}$$

Bringing Equations (5)–(8) into (4), the even-mode resonant frequencies can be deduced by solving $Y_{\text{in,even}} = 0$.

We can observe from formulas (3)–(8) the relationship between the resonator frequencies and the electrical length of each stub in a DTOS multimode resonator. The resonator odd mode frequency only has a relationship with θ_1, θ_2, and θ_s, but the even mode frequency has a relationship with θ_1, θ_2, θ_s, θ_3, θ_4, and θ_5. To put it another way, changing the physical lengths of l_3, l_4, and l_5 will only impact the even mode frequency of the DTOS multimode resonator; however, changing l_1, l_2, and l_s would change both the even and odd mode frequencies.

Figure 3 shows the frequency response of five resonant frequencies (f_{e1}, f_{e2}, f_{e3}, f_{o1}, f_{o2}) under weak coupling conditions ($l_6 = 1\,\text{mm}$, $w_6 = 0.2\,\text{mm}$). Figure 3(a) shows the frequency response of resonant frequency with l_1. Three even mode frequencies (f_{e1}, f_{e2}, f_{e3}) and two odd mode frequencies (f_{o1}, f_{o2}) shift to low frequencies as l_1 rises from 6.4 mm to 8.4 mm, with f_{o1}, f_{e2}, and f_{o2} showing the most pronounced shift range. Similarly, shifting l_2 physical length results in a change in each of the five resonant frequencies, as seen in Figure 3(b). Therefore, we may alter the odd and even mode frequencies by varying the lengths of l_1 and l_2. According to Figure 3(c), only the even mode frequencies (f_{e1}, f_{e2}, f_{e3}) move when the length of l_3 is altered, while the odd mode frequencies stay the same. Figure 3(d) makes it abundantly evident that altering the length of l_s allows us to suitably change the

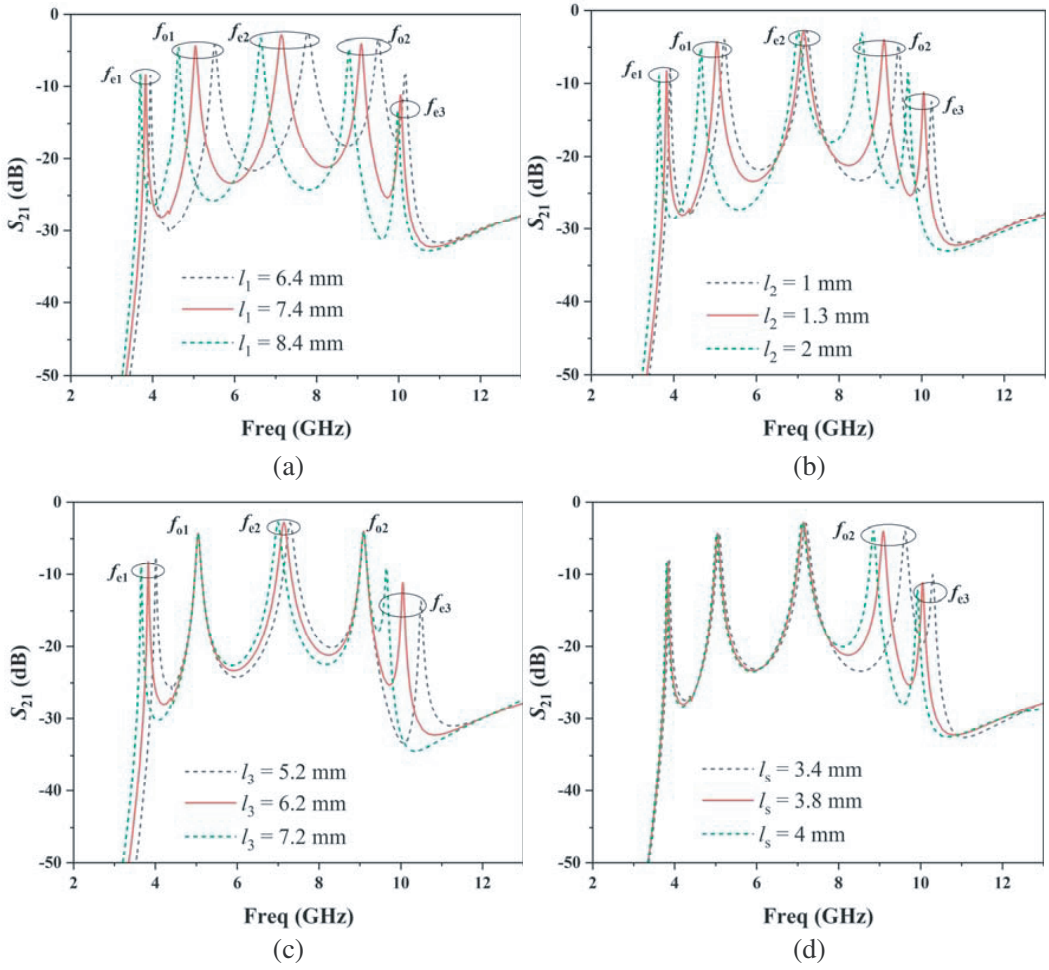

Figure 3. Frequency response under weak coupling. (a) l_l length variation. (b) l_2 length variation. (c) l_3 length variation. (d) l_s length variation.

even mode frequency (f_{e3}) and odd mode frequency (f_{o2}) located close to the upper stopband edge. This allows us to increase the upper edge of the bandwidth and increase the passband compliance with the UWB passband. The resonant frequencies may be simply assigned by appropriately altering the DTOS MMR's structural dimensions.

According to the research above, interdigital coupled lines may strengthen the MMR coupling to provide a flat passband [18]. Figure 4(a) compares the simulated transmission coefficient (S_{21}) of the filter under weak and strong coupling conditions. For this comparison, the coupling linewidth (w_6) is fixed at 0.2 mm. As the interdigital coupled lines length (l_6) increases from 1 mm to 7.4 mm, the five resonant frequencies (f_{e1}, f_{e2}, f_{e3}, f_{o1}, f_{o2}) gradually increase and are broadened into a passband response. At the same time, the passband flattens. Furthermore, two transmission zeros TZ_1 and TZ_2 emerge on either side of the passband because of the increased coupling strength. Here, for broad bandwidth and a flat passband, the coupling length $l_6 = 7.4$ mm must be in the range of $\lambda_g/4$ (where λ_g is the guided wavelength of the proposed filter at the center frequency). Considering manufacturing process issues, there is a 0.1 mm minimum distance between them.

Optimized by electromagnetic simulation software, Figure 4(b) depicts the final design of the proposed BPF after the parameter research. Due to the formation of two TZs at 2.73 GHz and 10.77 GHz, the S-parameter frequency response shows that the BPF filter has extremely strong selectivity. The needed passband's return loss must be less than 16 dB for the analog 3 dB passband, which spans the frequencies of 3.5 GHz to 10.1 GHz. The stopband has a minimum attenuation of −12 dB and extends to 20 GHz.

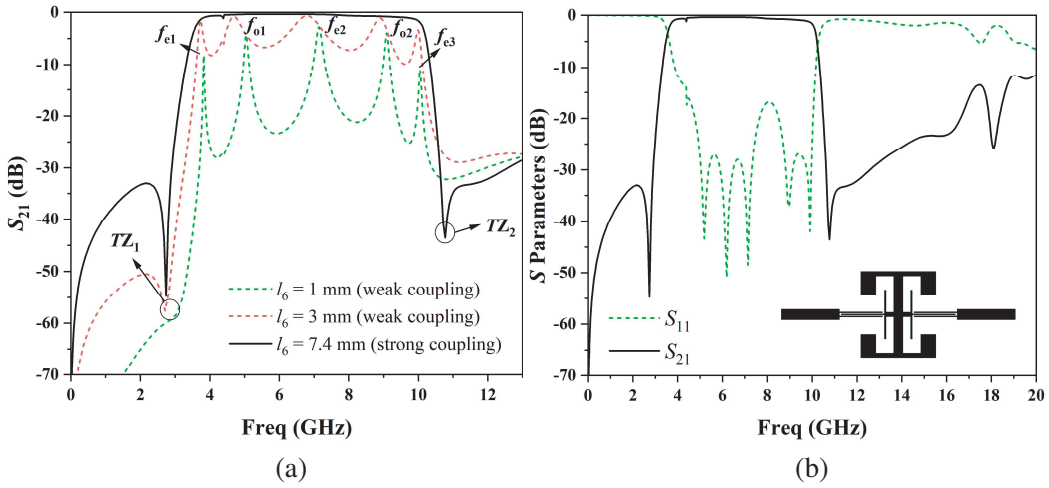

Figure 4. Frequency response. (a) Parameter simulation of varying l_6. (b) S-parameter simulation of the UWBBPF.

3. DUAL NOTCHES UWB FILTER

After the construction of the UWB filter, as previously explained, the placement of many stopbands inside the UWB passband has the ability to efficiently minimize a variety of in-band interferences that may result from the basic response. The dual notches bandpass filter that is being suggested features blocking bands at 5.8 and 8 GHz to prevent interference from WLAN and X-band narrowband RF signals, respectively. Utilizing CFSRR [19] (5.8 GHz) and FSRR [20] (8 GHz), these notches are produced. These resonators (CFSRR and FSRR) are positioned in pairs close to the input and output feedlines such that, at their respective resonant frequencies, they are the most active (i.e., have the greatest current density) parts of the notched filter. The location of these notched bands is related to the geometric length of the resonator by the following equation:

$$f(5.8\,\text{GHz}) \approx c/\left(2l_{\text{CFSRR}}\sqrt{\varepsilon_{\text{reff}}}\right) \tag{9}$$

$$f(8\,\text{GHz}) \approx c/\left(2l_{\text{FSRR}}\sqrt{\varepsilon_{\text{reff}}}\right) \tag{10}$$

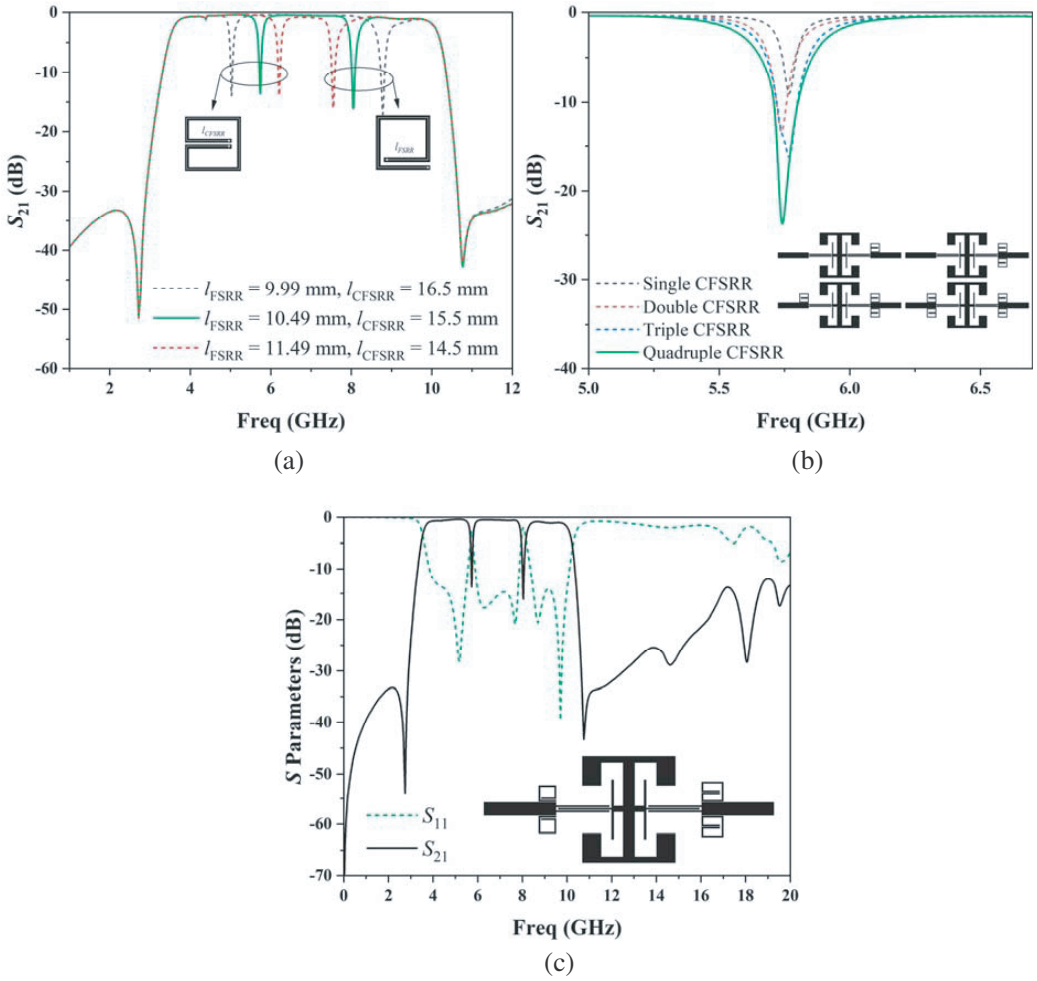

Figure 5. (a) Variation of notched frequencies for variable lengths of FSRR and CFSRR. (b) Bandwidth variation for different numbers of resonators CFSRRs. (c) Simulated frequency response of the proposed dual notched band filter.

where c is the velocity of light and $\varepsilon_{\text{reff}}$ (for 0.2 mm microstrip line) = 2.36.

The physical length of the two resonators can be adjusted to control the two notched frequencies, as illustrated in Figure 5(a), which shows the range of notched frequency variation resulting from changes in the lengths of the CFSRR and FSRR resonators. This flexibility makes it possible to move the dual notches to any desirable location within the UWB passband, thus removing undesired interference. The two resonator lengths may be determined as $l_{\text{CFSRR}} = 15.5$ mm and $l_{\text{FSRR}} = 10.49$ mm using Equations (9) and (1). Figure 5(a), which contains the graphs of the two resonators producing the notched characteristics, presents the response of the proposed multi-band notched bandpass filter. The two notches have attenuation depths of 13 and 16 dB and are placed at frequencies of 5.8 and 8 GHz, respectively. According to simulation findings, using pairs of resonators enhances the notched bandwidth and attenuation depth, as illustrated in Figure 5(b). Figure 5(c) displays the frequency response of the optimized final suggested filter. The current distribution of the filter at the two notched frequencies is shown in Figure 6 to further clarify the connection between the produced notched frequencies and the suggested notched construction. Indicating that these resonators are the main causes of notched generation inside the UWB passband, it is clear from the current density that it is concentrated in the CFSRRs and FSRRs at the 5.8/8 GHz frequency. The physical dimensions of the optimized dual notches UWB filter structure are as follows (all in mm): $w = 1.82$, $l_1 = 7.4$, $w_1 = 0.2$, $l_2 = 1.3$, $w_2 = 0.8$, $l_3 = 6.2$, $w_3 = 1.6$, $l_4 = 3.05$, $w_4 = 0.8$, $l_5 = 4$, $w_5 = 2.6$, $l_6 = 7.4$, $w_6 = 0.2$, $l_s = 3.8$, $w_s = 0.3$, $g_1 = 0.3$, $g_2 = 0.15$, $g_3 = 0.1$, $t_1 = 0.1$, $t_2 = t_3 = 0.2$, $l_{\text{CFSRR}} = 15.5$, $l_{\text{FSRR}} = 10.49$.

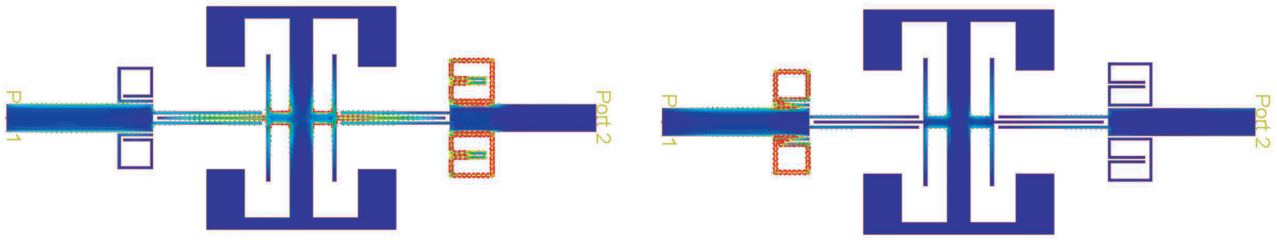

(a) 5.8 GHz (b) 8 GHz

Figure 6. Current distribution at: (a) The first notched band 5.8 GHz, (b) The second notched band 8 GHz.

4. EXPERIMENTAL VERIFICATION

An image of the manufacturing and examination of the prototype notched BPF may be seen in Figure 7. The filter is 40 mm × 18 mm overall (with two feedlines). Using the network analyzer ZNB40, we created and measured the suggested BPF RF device. Figure 8 illustrates a comparison between measured data and simulation findings. The measured passband width is 3.5–10.1 GHz, and return loss is better than 11 dB within the passband, as can be shown. The entire passband is divided into three passbands by the two notches, with the first passband located before the first notch at 5.8 GHz and having insertion loss less than 0.86 dB, the second passband located between the two notches and having insertion loss less than 1.3 dB, and the third passband located at the 3 dB cutoff frequency from the second notch at 8 GHz to the higher passband and having insertion loss less than 1.05 dB. In addition, the two notches attenuation is at least less than −14 dB. Up to 20 GHz, a 17 dB broad stopband is seen. Excluding the two notches, the passband group delay oscillates between 0.37 and 0.95 ns. A non-enclosed dielectric substrate, SMA joint loss, or artifactual soldering levels may be to blame for the disparity between the observed and simulated data. The findings of the comparison between the UWB filter developed in this publication and [11–13, 16, 17, 19, 20] are shown in Table 1. It can be seen from the last row of Table 1 that the structure proposed in this paper achieves excellent roll-off on both sides of the passband, compact size, and also achieves a wide stopband characteristic.

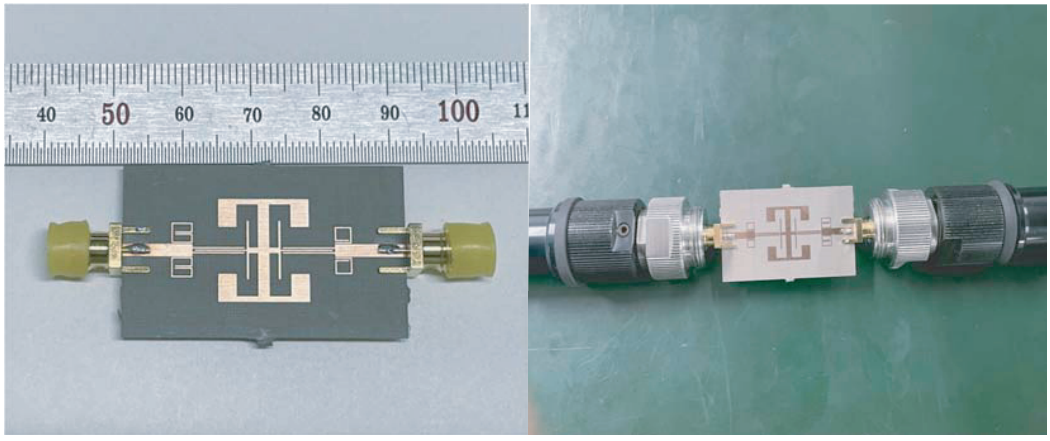

(a) (b)

Figure 7. The photographs of the proposed notch-band UWB-BPF. (a) Physical photo. (b) Test photo.

Table 1. A comparison between the proposed filter and other reported UWB filters.

Ref.	ε_r/height (mm)	Passband (GHz)	Notches (GHz)/ attenuation (dB)	S. F.*	Stopband (GHz)/ attenuation (dB)	size ($\lambda_g \times \lambda_g$)
[11]	2.2/0.787	3.4–10	5.2/> 22.7	0.66	19/> 11	0.70×0.28
[12]	2.55/0.8	3.1–10.6	5–6/> 12.5	0.789	27.6/> 20	0.514×0.312
[13]	3.38/0.508	3.04–10.78	5.8/> 17.9	0.703	11/> 15	0.87×0.66
[16]	2.2/0.787	3.14–10.53	5.13, 8/> 13	0.954	14/> 2	1.9×0.44
[17]	2.65/1.0	2.8–11.0	5.3, 7.8/> 20	0.781	30/> 15	1.12×0.61
[19]	4.4/0.8	2.5–10.96	5.1, 6.45, 7.9 > 18	0.821	16/> 15	0.95×0.78
[20]	10.2/0.635	2.9–10.75	5.13, 6.15, 8 > 18	0.765	15/> 15	0.95×0.78
This work	3.38/0.8	3.5–10.1	5.8, 8 > 16	0.857	20/> 20	0.55×0.75

* S. F: selectivity factor of the passband; S. F = $\Delta f_{3\,\mathrm{dB}}/\Delta f_{3\,\mathrm{dB}}$; where $\Delta f_{3\,\mathrm{dB}}$ and $\Delta f_{3\,\mathrm{dB}}$ are the bandwidth of the passband, respectively.

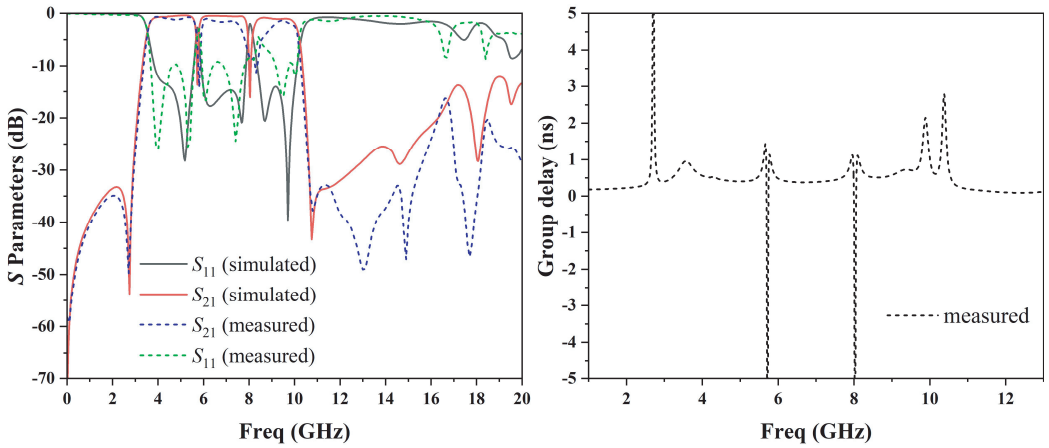

(a) (b)

Figure 8. Comparison of simulated and measured frequency responses. (a) S amplitude curve. (b) Measured group delay.

5. CONCLUSION

The article introduces a highly selective UWB-BPF with dual notched bands, which is composed of several components, including a double-T-shaped open stub-loaded MMR interdigital coupled lines and two pairs of complementary folded split ring resonators (CFSRRs) and folded split ring resonators (FSRRs) coupled near the feedlines. The proposed filter is promising for applications in UWB systems that require the suppression of interference from WLAN and X-band satellite communication signals. Because of its low cost, wide passband, and ultra-wide upper stopband, the filter could enable widespread adoption in UWB wireless communication systems.

REFERENCES

1. FCC, "Revision of part 15 of the commission's rules regarding ultra-wideband transmission system," *ET-Docket*, 98153, Washington, 2002.
2. Razzaz, F., S. M. Saeed, and M. A. S. Alkanhal, "Ultra-wideband bandpass filters using tapered resonators," *Applied Sciences*, Vol. 12, No. 7, 3699, 2022
3. Chu, Q.-X. and X.-K. Tian, "Design of UWB bandpass filter using stepped-impedance stub-loaded resonator," *IEEE Microwave and Wireless Components Letters*, Vol. 20, No. 9, 501–503, 2010, doi: 10.1109/LMWC.2010.2053024.
4. Kumari, P., P. Sarkar, and R. Ghatak, "Design of a compact UWB BPF with a fractal tree stub loaded multimode resonator," *IET Microwaves, Antennas & Propagation*, Vol. 15, No. 1, 5561, 2021.
5. Yao, B., Y. Zhou, Q. Cao, and Y. Chen, "Compact UWB bandpass filter with improved upper-stopband performance," *IEEE Microwave and Wireless Components Letters*, Vol. 19, No. 1, 27–29, 2009, doi: 10.1109/LMWC.2008.2008558.
6. Ghazali, A. N., M. Sazid, and B. Virdee "A compact UWB-BPF based on microstrip-to-CPW transition with multiple transmission zeros," *Microw. Opt. Technol. Lett.*, 60, 2018, https://doi.org/10.1002/mop.31274.
7. Sun, X. and E. L. Tan, "Novel ultra-wideband filter using coplanar-waveguide-to-microstrip transition and stubs," *Microw. Opt. Technol. Lett.*, Vol. 55, No. 10, 22692271, 2013, doi: 10.1002/mop.27870.
8. Ghazali, A. N., M. Sazid, and S. Pal, "A miniaturized microstrip-to-CPW transition based UWB-BPF with sharp roll-off and minimum insertion loss," *Microw. Opt. Technol. Lett.*, Vol. 58, No. 2, 289–293, 2016, doi:10.1002/mop.29551
9. Lin, H., X. Xia, Z. Guo, H. Jin, and T. Yang, "Compact high selectivity UWB filter using composite CPW-microstrip structure," *IEICE Electron. Exp.*, Vol. 13, No. 24, 16, 2016, doi: 10.1587/elex.13.20161049
10. Wang, Y. X., L. Zhu, and S. B. Zhang, "High-selective wideband bandpass filter with adjustable notched-band using stub-loaded resonator," *Electronics Letters*, Vol. 49, No. 24, 1542–1544, 2013.
11. Weng, M. H., C. W. Hsu, S. W. Lan, and R. Y. Yang, "An ultra-wideband bandpass filter with a notch band and wide upper bandstop performances," *Electronics*, Vol. 8, No. 24, 11.1316, 2019, doi: 10.3390/electronics8111316.
12. Zhu, H. and Q.-X. Chu, "Ultra-wideband bandpass filter with a notch-band using stub-loaded ring resonator," *IEEE Microwave and Wireless Components Letters*, Vol. 23, No. 7, 341–343, 2013, doi: 10.1109/LMWC.2013.2262928.
13. Li, J., C. Ding, F. Wei, and X. W. Shi, "Compact UWB BPF with notch band based on SW-HMSIW," *Electronics Letters*, Vol. 51, No. 17, 1338–1339, 2015
14. Ghazali, A. N., M. Sazid, and S. Pal, "A miniaturized low-cost microstrip-to-coplanar waveguide transition-based ultra-wideband bandpass filter with multiple transmission zeros," *Microwave Opt. Technol. Lett.*, Vol. 62, No. 12, 3662–3667, 2020.
15. Ghazali, A. N. and M. Sazid, "Design of multiple transmission zeros-enabled compact broadband BPFs based on microstrip-to-CPW transition technology," *International Journal of Microwave and Wireless Technologies*, Vol. 14, No. 5, 546552, 2022.
16. Sarkar, P., R. Ghatak, M. Pal, and D. R. Poddar, "High-selective compact UWB bandpass filter with dual notch bands," *IEEE Microwave and Wireless Components Letters*, Vol. 24, No. 7, 448–450, 2014, doi: 10.1109/LMWC.2014.2316214.
17. Song, Y., G.-M. Yang, and W. Geyi, "Compact UWB bandpass filter with dual notched bands using defected ground structures," *IEEE Microwave and Wireless Components Letters*, Vol. 24, No. 4, 230–232, 2014, doi: 10.1109/LMWC.2013.2296291.
18. Chen, C. P., N. Kato, and T. Anada, "Synthesis scheme for wideband filters consisting of three coupled-lines including the cross coupling between non-adjacent lines," *IET Microw. Antennas Propag.*, Vol. 9, No. 14, 1558–1566, 2015.

19. Sazid, M., N. S. Raghava, and A. N. Ghazali, "UWB-BPF based on broadside coupled technology with triple-notched passband," *Microw. Opt. Technol. Lett.*, Vol. 65, No. 7, 1910–1916, 2023.
20. Ghazali, A. N., M. Sazid, and S. Pal, "A surface-to-surface transition based UWB bandpass filter with triple in-band notches," *International Journal of Electronics and Communications*, Vol. 157, 154411, 2022.